Supplementary Information

Supplementary Figures 1–7

Supplementary Tables 1–5

Supplementary Video legends

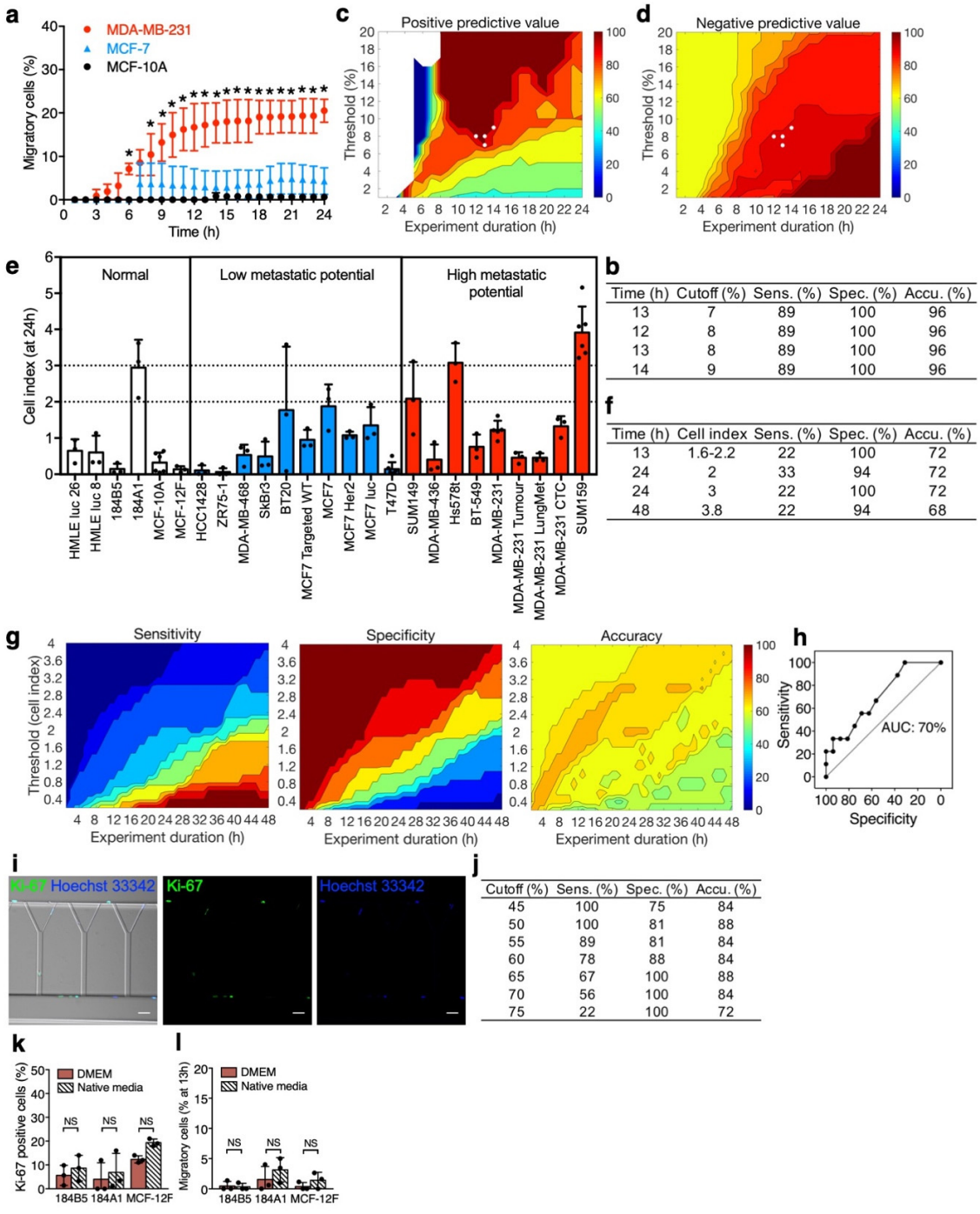

Supplementary Fig. 1 | Use of MAqCI for prediction of metastatic potential of breast epithelial and breast cancer cell lines. a, Percentage of migratory cells as a function of time in representative cell lines with high metastatic potential (MDA-MB-231), low metastatic potential (MCF-7), and normal-like breast epithelial cells (MCF-10A). Data represent mean±SEM from *n*=3 independent experiments. *, *p*<0.05 compared to MCF-10A and MCF-7,

as calculated by two-way ANOVA followed by Tukey's multiple comparisons test. Due to the large number of comparisons, exact *p*-values are listed in Supplementary Dataset 3. **b**, Combinations of threshold percentage of migratory cells and experiment duration that result in optimal accuracy for MAqCI based only on migration index. **c**, Positive predictive value (PPV, sum of true positive predictions divided by sum of assay positive predictions) and **d**, negative predictive value (NPV, sum of true negative predictions divided by sum of assay negative predictions) of predictions based on migration index as a function of experiment duration and threshold percentage. At early time points, the assay makes no positive predictions and PPV is undefined (white region). White circles represent the values corresponding to optimal accuracy (96%). **e**, Cell index (proxy for number of cells that migrated) at 24 h of breast epithelial and breast cancer cell lines measured in a transwell-migration assay using the xCELLigence RTCA DP instrument with CIM-plate 16 chambers. Each data point represents the cell index from 1 experiment, averaged from 3 technical replicates. Column and error bars represent mean±SD of n≥3 independent experiments. Dotted lines designate cell index of 2 and 3. **f**, Combinations of threshold cell index and experiment duration that result in maximal accuracy of prediction of metastatic potential of established cell lines based on the mean cell index from the transwell-migration assay. **g**, Sensitivity, specificity and accuracy (%) of prediction of metastatic potential of established cell lines based on the mean cell index from the transwell-migration assay. Metrics are calculated as a function of experiment duration (0-48h) and threshold cell index (0-4) above which a cell line is predicted to have high metastatic potential. **h**, ROC of metastatic potential predictions based on cell index from the transwell-migration assay. **i**, MDA-MB-231 cells in MAqCI after immunostaining for Ki-67 and the nucleus (Hoechst 33342). Scale bars, 50μm. **j**, Prediction sensitivity, specificity and accuracy based on proliferation index only at different threshold values of percent Ki-67-positive cells. **k**, Percentage of Ki-67-positive cells or **l**, migratory cells at 13h observed in MAqCI filled with DMEM+10%FBS+1%P/S (DMEM) versus each cell line's native media (listed in Materials and Methods). Columns and error bars represent mean±SD of n=3 independent experiments. *P*-values calculated by one-way ANOVA followed by Tukey's multiple comparisons test. Due to the large number of comparisons, exact *p*-values are listed in Supplementary Dataset 3.

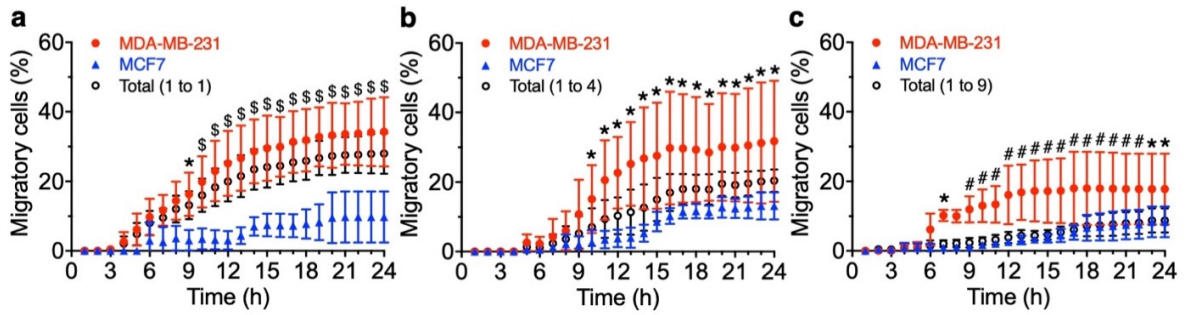

Supplementary Fig. 2 | Identification of migratory cells within heterogeneous cell populations. Percentage of migratory cells from mixed populations of MDA-MB-231 and MCF7 cells pre-labeled with two spectrally distinct fluorophores. Fluorescent cell labelling allowed each cell line to be analyzed individually, as well as the mixed population. Data represent mean±SD from *n*=3 independent experiments. A total of 50,000 cells were seeded in each device, at ratios of **a**, 1:1 MDA-MB-231 cells to MCF7 cells **b**, 1:4 **c**, 1:9. *P*-values calculated by two-way ANOVA followed by Tukey's multiple comparisons test. *, $p<0.05$ for MDA-MB-231 compared to MCF7 at the same time point. $, $p<0.05$ for MDA-MB-231 and Total compared to MCF7. #, $p<0.05$ for MDA-MB-231 compared to MCF7 and Total. Due to the large number of comparisons, exact *p*-values are listed in Supplementary Dataset 3.

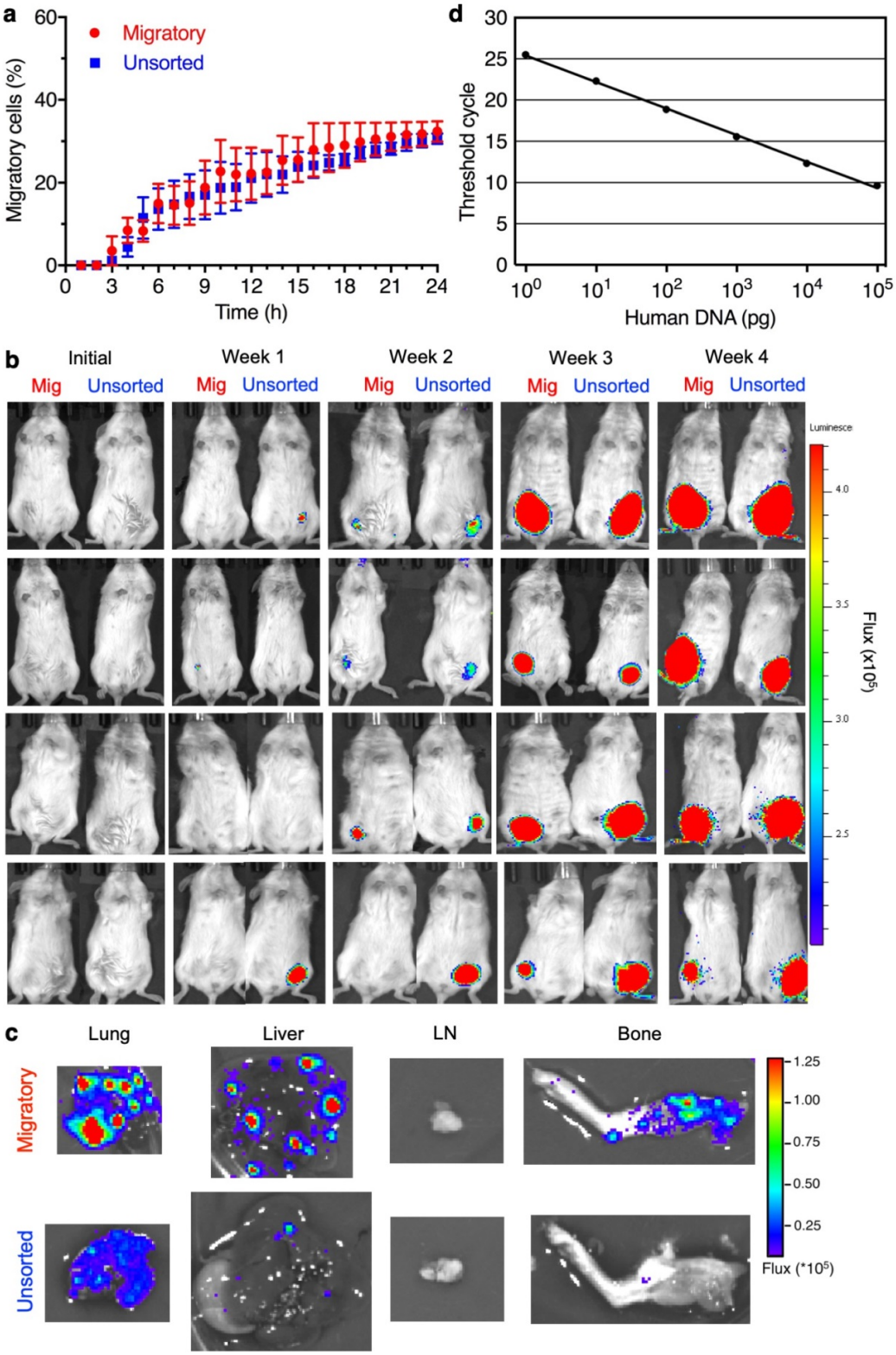

Supplementary Fig. 3 | Migratory cells have enhanced metastatic, but not tumourigenic, potential *in vivo* compared to unsorted breast cancer cells. a, Percentage of migratory cells

from migratory and unsorted MDA-MB-231 populations cultured for 14 days after isolation from MAqCI. Data represent mean±SEM from *n*=3 independent experiments. **b**, Representative bioluminescent images of tumour growth in mice injected with migratory or unsorted MDA-MB-231 cells. **c**, Additional representative bioluminescent images of the lung, liver, axillary lymph node (LN), and bone of mice injected with migratory or unsorted cells (8 images acquired per condition, see also Fig. 2b). **d**, Standard curve for threshold cycle detection of human DNA isolated from MDA-MB-231 cells and detected using qPCR. For each experiment, the average value of three technical replicates was used. Data represent mean±SEM from *n*=3 independent experiments. Line represents best fit, R^2>0.99 as calculated by linear trendline in Microsoft Excel.

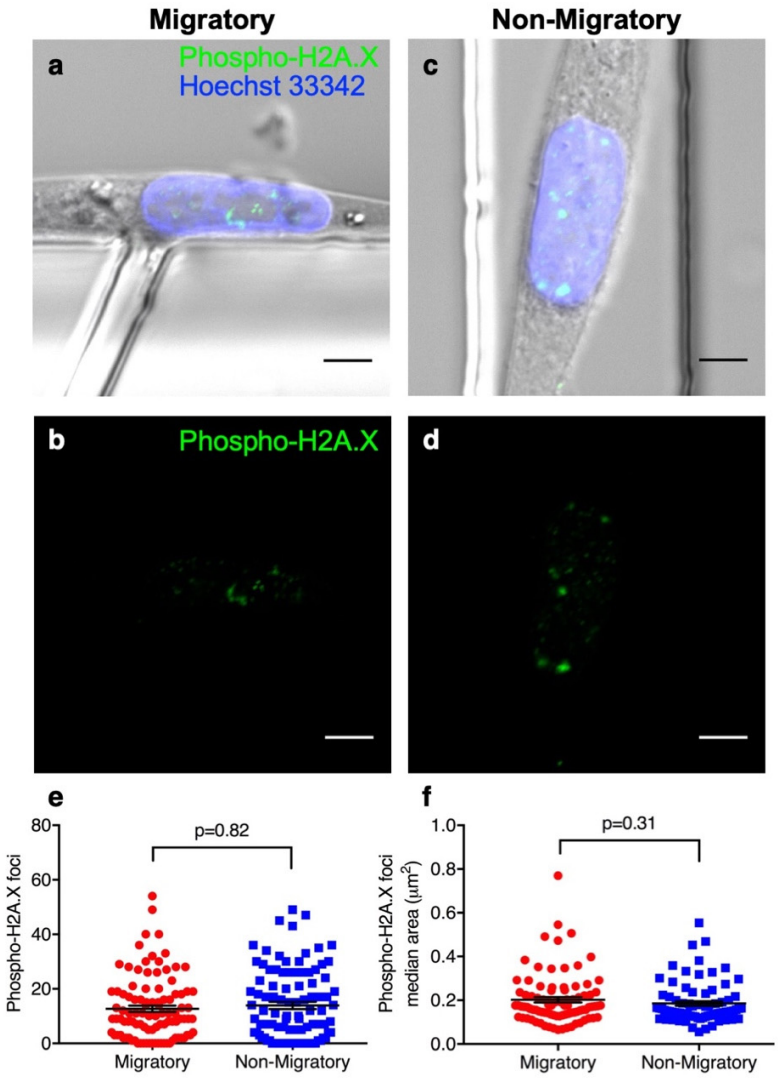

Supplementary Fig. 4 | Cell entry and migration inside the narrower branch channels do not induce DNA damage. a-b, Migratory and **c-d**, non-migratory MDA-MB-231 cells immunostained for phospho-H2A.X and the nucleus (Hoechst 33342) after migration in MAqCI. Scale bars, 5μm. **e**, Number and **f**, median area of phospho-H2A.X foci identified in the nucleus of migratory and non-migratory cells. Error bars represent mean±SEM of data pooled from *n*=4 independent experiments. *P*-values calculated by two-tailed Mann-Whitney test.

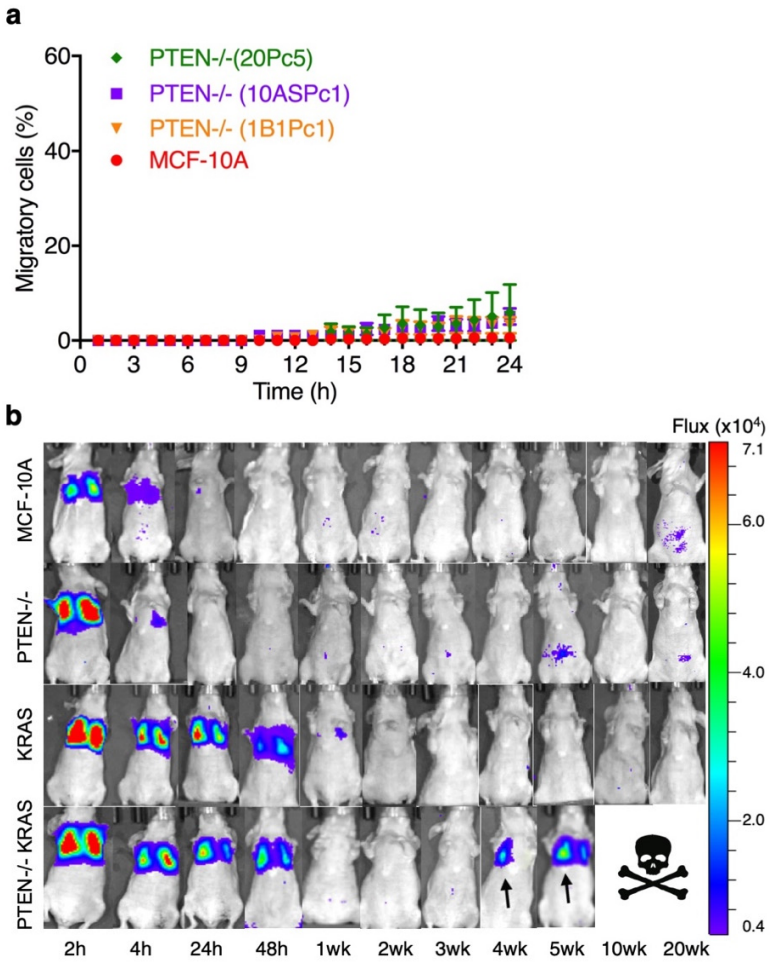

Supplementary Fig. 5 | MAqCI predicts metastatic potential conferred by activation of PI3K and Ras/MAPK pathways in breast epithelial cells. a, Percentage of migratory cells in different PTEN-/- clones compared to the parental MCF-10A population. Data represent mean±SEM from $n \geq 3$ independent experiments. Data plotted here for clone 20Pc5 is also shown in Fig. 4a and this clone was used for all other experiments. **b**, Additional representative bioluminescent images of mice following tail vein injection with 10^6 cells (5 animals imaged per group, see also Fig. 4d). PTEN-/-KRAS(G12V) cells form tumours (arrows) causing ethical endpoint before 20 weeks.

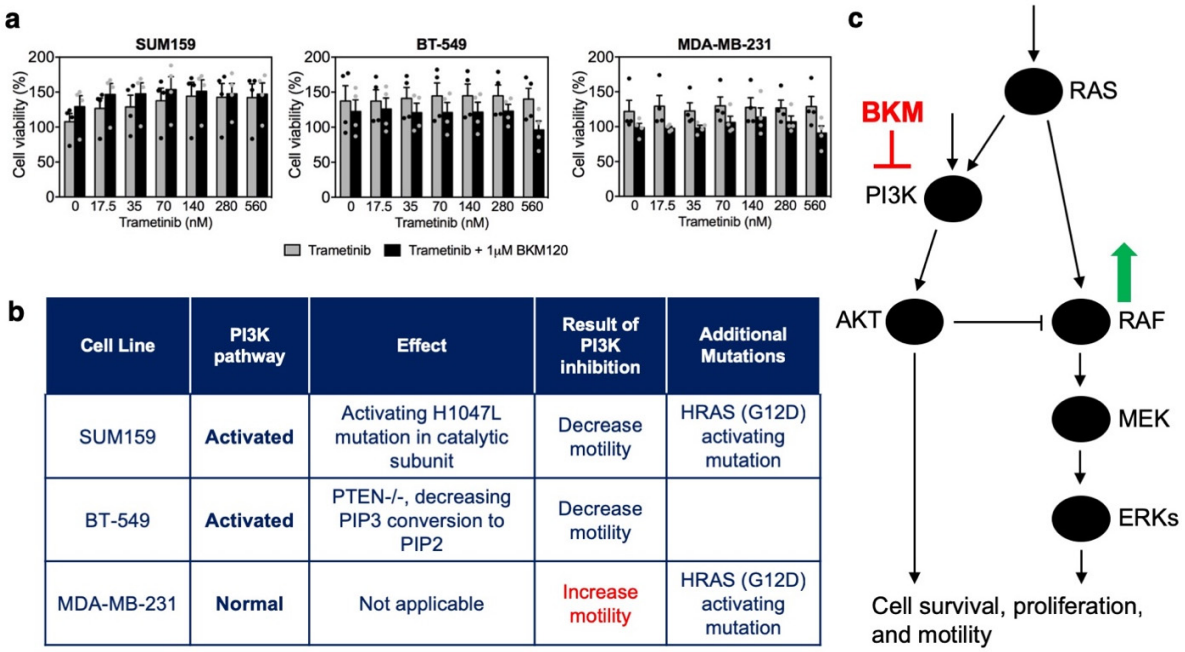

Cell Line	PI3K pathway	Effect	Result of PI3K inhibition	Additional Mutations
SUM159	**Activated**	Activating H1047L mutation in catalytic subunit	Decrease motility	HRAS (G12D) activating mutation
BT-549	**Activated**	PTEN-/-, decreasing PIP3 conversion to PIP2	Decrease motility	
MDA-MB-231	**Normal**	Not applicable	Increase motility	HRAS (G12D) activating mutation

Supplementary Fig. 6 | MAqCI testing of therapeutic agents from ongoing clinical trials. a, Cell viability for SUM159, BT-549, and MDA-MB-231 cells treated with trametinib for 24h relative to vehicle control treated cells. Select samples were also treated with BKM120 (1μM). Each data point represents the percentage from 1 experiment. Column and error bars represent mean±SEM of n≥3 independent experiments. **b**, PI3K pathway genotype for SUM159, BT-549 and MDA-MB-231 cell lines and the effect of PI3K inhibition on their motility. **c**, Mechanism for RAF activation during PI3K inhibition.

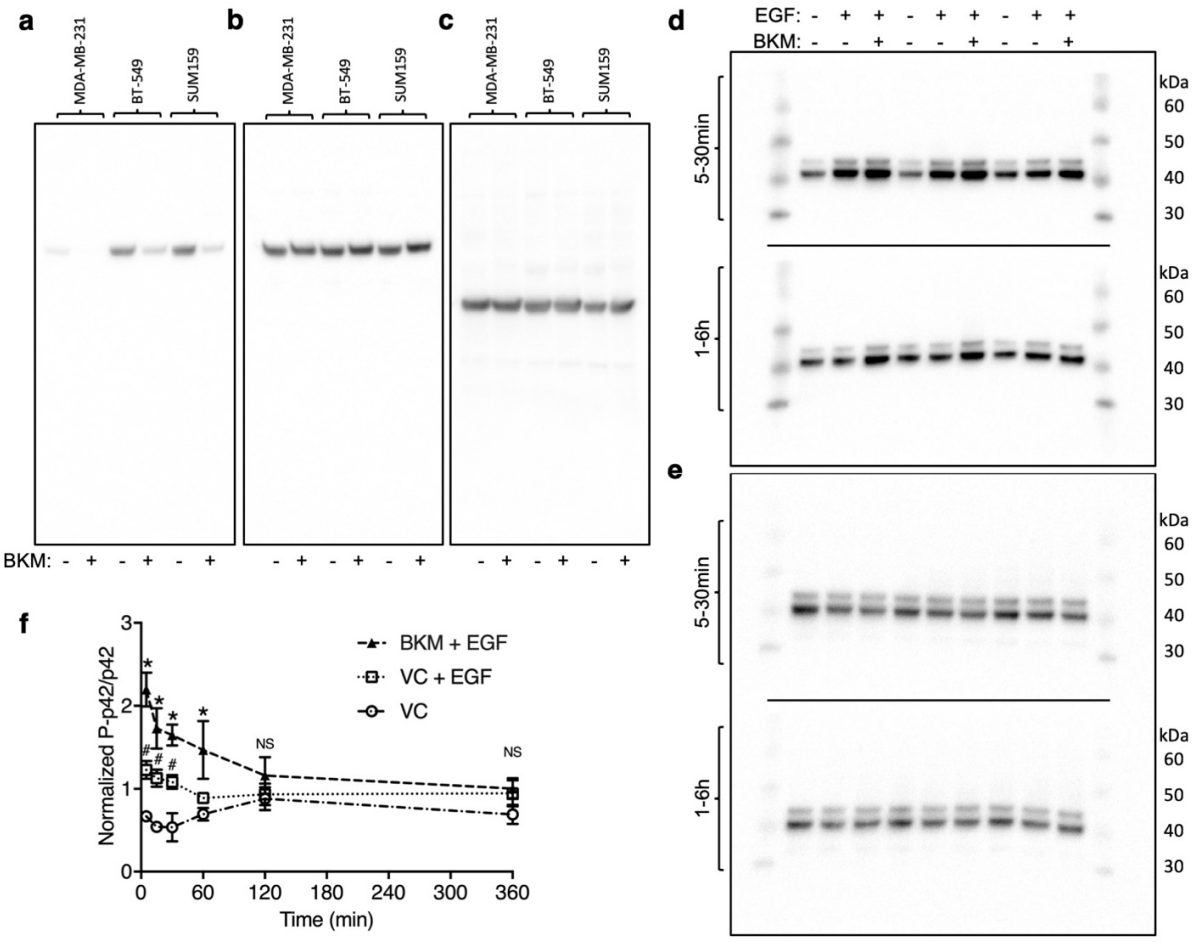

Supplementary Fig. 7 | PI3K and RAS/MAPK signaling in triple negative breast cancer cell lines. Representative western blot for **a**, pAKT (Ser473), **b**, Total AKT and **c**, actin in MDA-MB-231, BT-549, and SUM159 cells treated with vehicle control or BKM120 (1μM) for 24h. Cropped versions of these scans appear in Figure 6g. **d**, Representative western blot for pERK and **e**, total ERK in MDA-MB-231 cells serum-starved for 24h, treated with vehicle control or BKM120 (1μM) for 30min, then in select samples stimulated with EGF (100nM) for the indicated time. Horizontal lines denote separation between two membranes that were processed and imaged in parallel. Cropped versions of these scans appear in Figure 6h. **f**, Quantification of western blots for pERK and total ERK (representative images shown in Figure 6h). Data represent the mean±SEM of densitometry measurements from three independent experiments. *, $p<0.05$ for BKM + EGF compared to VC + EGF and VC; #, $p<0.05$ for VC + EGF compared to VC. NS, $p\geq0.05$. *P*-values calculated by two-way ANOVA followed by Tukey's multiple comparisons test. Due to the large number of comparisons, exact *p*-values are listed in Supplementary Dataset 3.

Supplementary Table 1 | Panel of established normal-like breast epithelial and breast cancer cell lines with either low or high metastatic potential used to validate MAqCI. Estrogen receptor (ER), progesterone receptor (PR), and Her2 status are indicated. Mean percentage of migratory and Ki-67-positive cells from $n \geq 3$ independent experiments. Probability (P) of having high metastatic potential calculated with logistic regression formula using migration and proliferation indices as predictors.

	Cell line	Disease	Site of origin	ER	PR	Her2	% mig	% Ki67	P
Normal	HMLE luc 26	None	Mammary gland/epithelium	Neg	Neg	Neg	0.5	48.4	0.00
	HMLE luc 8	None	Mammary gland/epithelium	Neg	Neg	Neg	1.6	33.1	0.00
	184B5	None	Mammary gland/epithelium	Neg	Neg	Neg	1.5	2.0	0.00
	184A1	None	Mammary gland/epithelium	Neg	Neg	Neg	5.7	0.0	0.00
	MCF-10A	Fibrocystic disease	Mammary gland	Neg	Neg	Neg	1.1	32.9	0.00
	MCF-12F	Fibrocystic disease	Mammary gland	Neg	Neg	Neg	3.3	32.6	0.00
Low metastatic potential	HCC1428	Adenocarcinoma	Metastatic site: pleural effusion	Pos	Pos	Neg	0.0	27.7	0.00
	ZR75-1	Ductal carcinoma	Metastatic site: ascites	Pos	Neg	Neg	0.0	25.1	0.00
	MDA-MB-468	Adenocarcinoma	Metastatic site: pleural effusion	Neg	Neg	Neg	0.0	62.0	0.00
	SkBr3	Adenocarcinoma	Metastatic site: pleural effusion	Neg	Neg	Pos	0.0	21.8	0.00
	BT20	Carcinoma	Primary tumor	Neg	Neg	Neg	0.0	33.4	0.00
	MCF7 Targeted WT	Adenocarcinoma	Metastatic site: pleural effusion	Pos	Pos	Neg	1.2	59.6	0.00
	MCF7	Adenocarcinoma	Metastatic site: pleural effusion	Pos	Pos	Neg	2.9	47.5	0.00
	MCF7 Her2	Adenocarcinoma	Metastatic site: pleural effusion	Pos	Pos	Neg	5.4	62.6	0.00
	MCF7 luc	Adenocarcinoma	Metastatic site: pleural effusion	Pos	Pos	Neg	6.5	38.5	0.00
	T47D	Ductal carcinoma	Metastatic site: pleural effusion	Pos	Pos	Neg	4.2	21.3	0.00
High metastatic potential	SUM149	Inflammatory ductal carcinoma	Primary tumor	Neg	Neg	Neg	1.2	71.5	1.00
	MDA-MB-436	Adenocarcinoma	Metastatic site: pleural effusion	Neg	Neg	Neg	8.7	62.5	1.00
	Hs578t	Carcinoma	Primary tumor	Neg	Neg	Neg	15.8	57.3	1.00
	BT-549	Ductal carcinoma	Primary tumor	Neg	Neg	Neg	17.5	56.0	1.00
	MDA-MB-231	Adenocarcinoma	Metastatic site: pleural effusion	Neg	Neg	Neg	17.2	92.6	1.00
	MDA-MB-231 Tumour	Adenocarcinoma	Xenograft - mammary fat pad	Neg	Neg	Neg	15.4	74.1	1.00
	MDA-MB-231 LungMet	Adenocarcinoma	Xenograft - lung metastases	Neg	Neg	Neg	24.8	74.7	1.00
	MDA-MB-231 CTC	Adenocarcinoma	Xenograft - CTC	Neg	Neg	Neg	46.3	77.2	1.00
	SUM159	Carcinoma	Primary tumor	Neg	Neg	Neg	29.9	89.4	1.00

Supplementary Table 2 | Logistic regression coefficients developed from panel of breast epithelial and breast cancer cell lines.

Feature	Logistic regression coefficient
Constant term (B0)	-2846
Migratory cells (%)	37.82
Ki-67 positive cells (%)	41.72

Supplementary Dataset 1 | Genes upregulated by migratory compared to unsorted MDA-MB-231 cells. Provided as a supplementary excel file.

Supplementary Dataset 2 | Genes downregulated by migratory compared to unsorted MDA-MB-231 cells. Provided as a supplementary excel file.

Supplementary Dataset 3 | Statistical tests. Description of statistical testing performed. Provided as a supplementary excel file.

Supplementary Video 1 | Definition of migratory and non-migratory cells in MAqCI. Migratory MDA-MB-231 cells (left) move through the feeder channel and enter one of the branch channels. Migration of non-migratory cells (right) is confined to the seeding area and the feeder channel. Cells were monitored by time-lapse microscopy in 20min intervals. Timestamp, h:min.

Supplementary Video 2 | Non-migratory MCF7 breast cancer cells in MAqCI. Representative examples of non-migratory MCF7 cells that do not reach (left) or fail to enter the branch channels (center, right). Cells were monitored by time-lapse microscopy in 20min intervals. Timestamp, h:min.

Supplementary Video 3 | Migration of breast cancer cells obtained from patient-derived xenografts in MAqCI. Cells were monitored by time-lapse microscopy in 20min intervals. Timestamp, h:min.